BRAHMS Overview

Ramiro Debbe† for the BRAHMS Collaboration

† Brookhaven National Laboratory, Upton NY, 11973

Abstract. A brief review of BRAHMS measurements of bulk particle production in RHIC Au+Au collisions at $\sqrt{s_{NN}} = 200 GeV$ is presented, together with some discussion of baryon number transport. Intermediate p_T measurements in different collision systems (Au+Au, d+Au and p+p) are also discussed in the context of jet quenching and saturation of the gluon density in Au ions at RHIC energies. This report also includes preliminary results for identified particles at forward rapidities in d+Au and Au+Au collisions.

1. Introduction

The vast majority of particles produced in high energy hadron collisions (pp, AA) have transverse momenta with steeply falling distributions and consists mostly of pions. This bulk particle production is often refered to as "soft physics"; an up to now intractable non-perturbative domain of QCD that remains poorly understood. Even though these collisions can be modeled with varying degrees of accuracy, a solution from "first principles" is still being sought. The BRAHMS collaboration at RHIC has set out to measure the bulk particle production in as wide as possible range in rapidity with good particle identification and high momentum resolution. The wide rapidity range offers an almost complete coverage that allows for the inclusion of conservation laws whenever a description of the physics behind the collisions is proposed. This contribution starts with a brief summary of some of BRAHMS most relevant measurements of bulk particle production.

The production of jets at RHIC energies is well established and, one of the most dramatic discoveries in Au+Au collisions at full energy has been the suppression of those jets as they traverse a highly opaque medium formed by the collisions [1, 2]. Studies of jet production with the BRAHMS apparatus are done through the measurement of leading particles up to intermediate values of transverse momentum ($\sim 4 GeV/c$). Our ability to identify the particles we measure, together with our high rapidity reach, make BRAHMS intermediate p_T measurements very relevant to study the longitudinal component of the new medium formed in Au+Au collisions. The high rapidity reach has also been instrumental in the study of charged particle production in d+Au collisions compared to incoherently added p+p collisions. The evolution of this comparison with rapidity and the centrality of the collision will be reviewed in this presentation. Finally, preliminary results from the analysis of Au+Au and d+Au collisions are presented in the last section. More details about BRAHMS results can be found in our "white paper" [3].

2. Experimental setup

The BRAHMS setup consists of two rotatable spectrometers, the mid-rapidity spectrometer (MRS) and the forward spectrometer (FS), complemented with an event characterization

system used to determine the geometry of the collisions. The MRS spectrometer measures the momentum of charged particles with two tracking stations (time projection chambers) and a single dipole magnet. Particle identification in this spectrometer is done with time-of-flight hodoscopes and a threshold Cherenkov detector. Details about the performance of the MRS spectrometer can be found in Ref. [4]. The FS spectrometer measures the much higher momenta of charged particles produced at small angles with five tracking stations (two TPC and three drift chambers). Particle identification in the FS spectrometer is done with a complement of two time-of-flight hodoscopes, one threshold Cherenkov counter and a Ring Imaging Cherenkov detector. A detailed description of the BRAHMS experimental setup can be found in [5]. The geometry of the collisions is extracted from the multiplicity of charged particles measured in the $|\eta| \leq 2.2$ range [6]. The normalization of our measurements is obtained with minimum biased triggers designed to maximize the coverage of the inelastic cross section. In Au+Au collisions that trigger was defined with the Zero Degree Calorimeters, ZDC, and for the p+p and d+Au collisions, with a set of scintillators located around the beam pipe.

3. Rapidity densities

The rapidity densities for the most central data sample $(0 - 5\%)$ in Au+Au collisions at $\sqrt{s_{NN}} = 200 GeV$ have been obtained by integration of the invariant differential yields $\frac{1}{2\pi} \frac{d^2 N}{p_T dp_T dy}$ at several intervals of rapidity. The measurement of very low values of transverse momentum p_T is limited by multiple scattering and particle decay, an interpolation is thus necessary in order to integrate the yields all the way down to zero p_T. Power law functions were used to integrate the pion distributions and single exponentials in $m_T - m_0$ for the kaon distributions [7]. Protons were fitted with single gaussians [8]. The result of these integrals is shown in Fig. 1. The shape of the produced particle densities (pions, kaons and anti-protons) is remarkably Gaussian. The width of the negative pion distribution is equal to: $\sigma_{\pi^-} = 2.29 \pm 0.02$. The widths of the rapidity densities of pions, kaons and anti-protons are very similar, and at the same time different from the ones associated with a single thermal source. A hydrodynamical description of the system is considered as the best approach to explain this wide distributions, even though hydrodynamical models [9], have not yet been able to reproduce the rapidity dependence of the so called elliptic flow [10].

Panel c of Fig. 1 shows the measured rapidity density for protons and anti-protons and panel d shows the net-proton density as function of rapidity after corrections from hyperon feed down. From this measurement an average rapidity loss of 2 units of rapidity has been deduced. The fact that the net proton yield around mid-rapidity is considerably different from zero, suggests that there are other mechanisms, besides valence quark transport that can move baryon number to mid-rapidity. Baryon junctions are considered as good candidates because their small-x component would be a natural way to place finite baryon number at $y \sim 0$ [11]. More details of this measurement can be found in ref. [8].

With the measurements described above, there is enough information to do an energy balance of the Au+Au collisions at $\sqrt{s_{NN}} = 200 GeV$. With reasonable assumptions about the particles that were not measured, and allowing for some $10 - 15\%$ error in the extrapolation up to beam rapidity, we find that 25 TeV out of the 33 TeV of total energy is found in produced particles. The integrated energy of the extrapolated net baryon distribution has been found to be $27 \pm 6\ GeV$ (see Ref. [8]), leaving $73 \pm 6\ GeV$, out of the 100 GeV of each incoming nucleon, available for particle production, well in agreement with the result obtained from the energy balance per particle species.

4. Intermediate p_T studies and the nuclear modification factors

As mentioned above, one of the most important results from RHIC is the suppression of intermediate p_T compared to appropriately scaled p+p collisions [1, 2]. Such reduction in
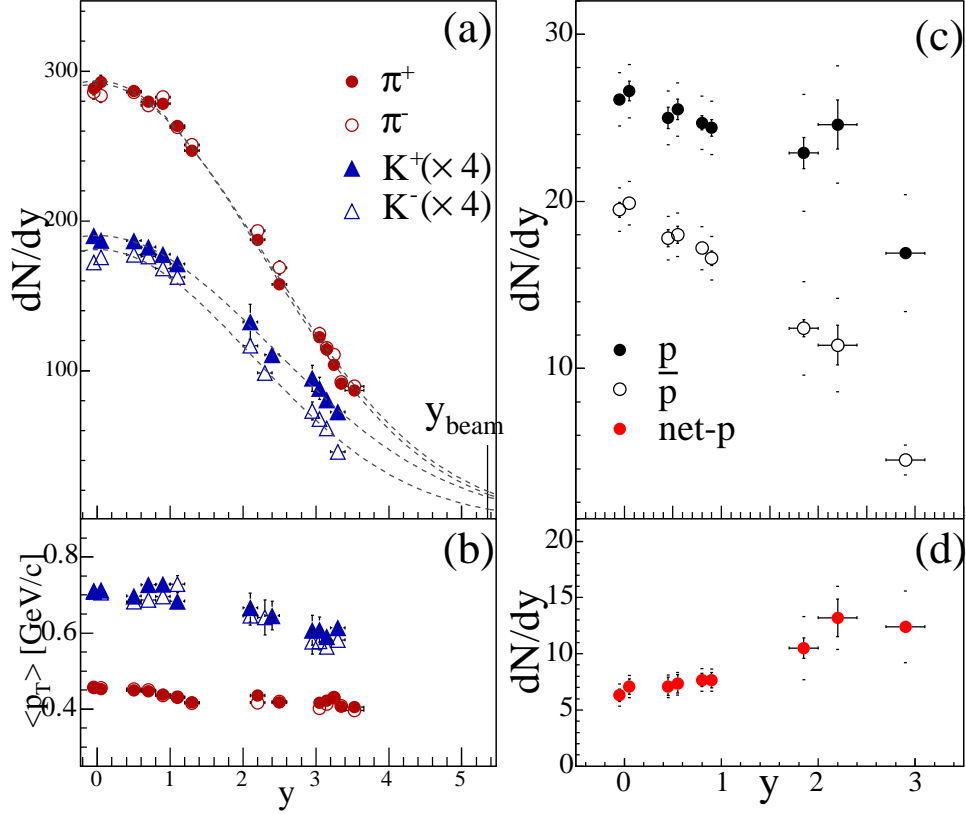
Figure 1. (a) Rapidity densities for pions and kaons. (b) Mean transverse momentum for pions, kaons and protons. (c) Rapidity density of protons and anti-protons. (d) Net proton rapidity densities corrected for hyperon feed-down. Small horizontal lines are used to display the systematic errors for the measurements displayed in panels c and d.

yield was soon identified as energy loss in a dense and opaque medium; partons with high fractional momentum traverse that medium while their energy is being degraded by multiple interactions (mainly gluon bremsstrahlung) and later hadronize into jets whose leading particles are then detected. Similar measurements performed in d+Au collisions at the same energy did not show the same strong suppression at mid-rapidity but rather an enhancement [12, 2]. This enhancement is understood as multiple elastic scatterings at the partonic level before the interactions that produce the jets whose leading particles are detected. The dominant source of the suppression measured in Au+Au collisions would then be the final state interactions with the opaque medium formed at the collision. BRAHMS extended a similar study to higher values of rapidity and found that the description of the enhancement measured at mid-rapidity in d+Au collisions was not applicable at forward rapidities, where in fact, we found again a suppression [13].

Figure 2 shows the nuclear modification factor defined as $R_{dAu} = \frac{1}{N_{coll}} \frac{\frac{dN^{dAu}}{dp_T d\eta}}{\frac{dN^{pp}}{dp_T d\eta}}$, where N_{coll} is the number of binary collisions estimated to be equal to 7.2 ± 0.6 for minimum biased d+Au collisions. Each panel shows the ratio calculated at a different η value. At mid-rapidity ($\eta = 0$), the nuclear modification factor exceeds 1 for transverse momenta greater than 2 GeV/c in a similar, although less pronounced way as Cronin's p+A measurements performed at lower
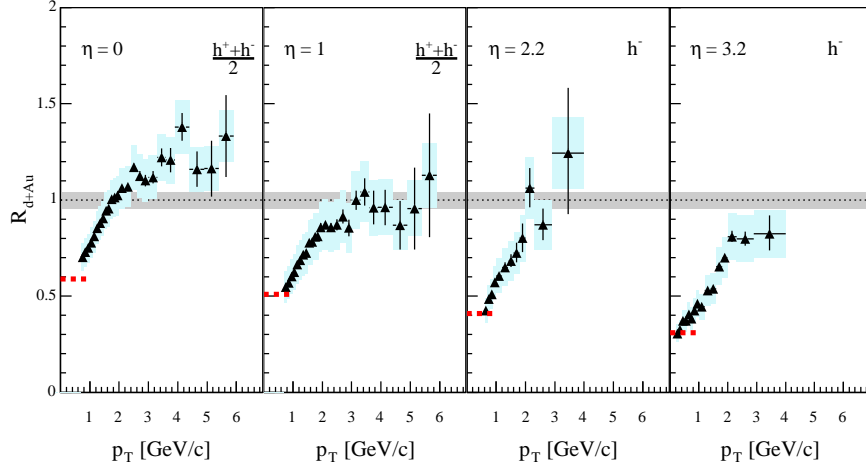
Figure 2. Nuclear modification factor for charged hadrons at pseudorapidities $\eta = 0, 1.0, 2.2, 3.2$. Statistical errors are shown with error bars. Systematic errors are shown with shaded boxes with widths set by the bin sizes. The shaded band around unity indicates the estimated error on the normalization to $\langle N_{coll} \rangle$. Dashed lines at $p_T < 1$ GeV/c show the normalized charged particle density ratio $\frac{1}{\langle N_{coll} \rangle} \frac{dN/d\eta(d+Au)}{dN/d\eta(pp)}$.

energies [14].

A shift of one unit of rapidity is enough to make the Cronin type enhancement disappear, and as the measurements are done at higher rapidities, the ratio becomes consistently smaller than 1 indicating a suppression in d+Au collisions compared to scaled p+p systems at the same energy.

In all four panels, the statistical errors, shown as error bars (vertical lines), are dominant specially in our most forward measurements. Systematic errors are shown as shaded rectangles. An additional systematic error is introduced in the calculation of the number of collisions N_{coll} that scales the d+Au yields to a nucleon-nucleon system. That error is shown as a 15% band at $R_{dAu} = 1$.

The four panels of Fig. 3 show the central $R_{CP}^{central}$ (filled symbols) and semi-central $R_{CP}^{semi-central}$ (open symbols) ratios for the four η settings. The evolution as function of rapidity seen in this figure is more obvious for samples of central events. Starting on the left panel corresponding to $\eta = 0$, the central events yields are systematically higher than those of the semi-central events, but at the highest pseudo-rapidity $\eta = 3.2$, the yields of central events are $\sim 60\%$ lower than the semi-central events for all values of transverse momenta. These results have generated much interest in the community because they appear as another indication of the onset of the so called Color Glass Condensate [15] at RHIC energies and high atomic numbers (A=179 for the gold ions) [16].

The analysis of the BRAHMS data collected from d+Au and p+p collisions is currently in progress, in particular, Fig. 4 presents the minimum bias nuclear modification R_{dAu} for anti-protons and negative pions at $\eta = 3.2$. The extraction of these ratios involved the following assumptions: at each p_T bin, one can extract the nuclear modification factor for identified particles, by multiplying the numerator and the denominator of this factor by the fractions of raw counts of identified particles to raw counts of negative particles for d+Au and p+p systems respectively:
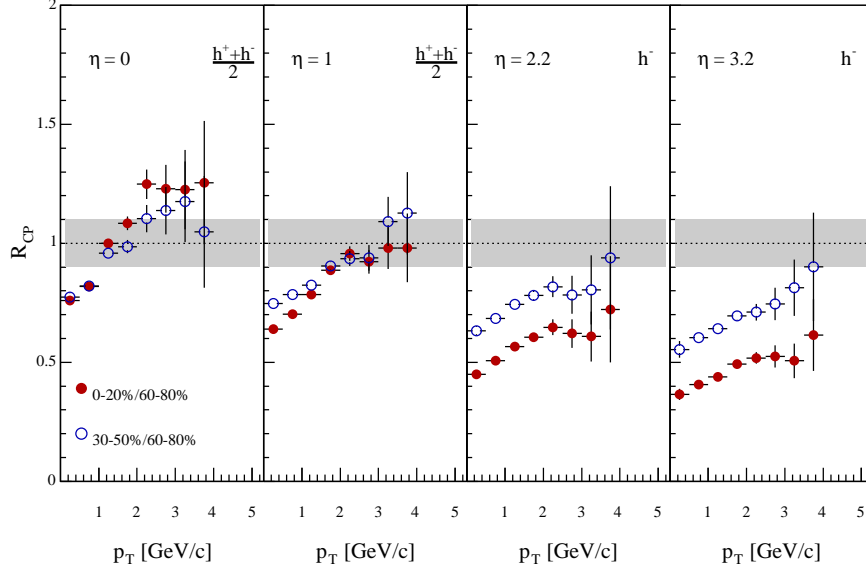
Figure 3. Central (full points) and semi-central (open points) R_{cp} ratios (see text for details) at pseudorapidities $\eta = 0, 1.0, 2.2, 3.2$. Systematic errors ($\sim 5\%$) are smaller than the symbols. The ratios at the highest pseudorapidities ($\eta = 2.2$ and 3.2) are calculated for negative hadrons. The uncertainty on the normalization of the ratios is displayed as a shaded band around unity. Its value has been set equal to the error in the calculation of N_{coll} in the most peripheral collisions (12%).

$$R_{dAu}^{\bar{p}} = R_{dAu}^{h^-} \frac{(\frac{\bar{p}}{h^-})^{dAu}}{(\frac{\bar{p}}{h^-})^{pp}} = \frac{1}{N_{coll}} \frac{\frac{dn^{dAu}}{dp_T d\eta}\Big)^{h^-}}{\frac{dn^{pp}}{dp_T d\eta}\Big)^{h^-}} \frac{\frac{\frac{dn^{dAu}}{dp_T d\eta}\Big)^{\bar{p}}}{\frac{dn^{dAu}}{dp_T d\eta}\Big)^{h^-}}}{\frac{\frac{dn^{pp}}{dp_T d\eta}\Big)^{\bar{p}}}{\frac{dn^{pp}}{dp_T d\eta}\Big)^{h^-}}} = \frac{1}{N_{coll}} \frac{\frac{dn^{dAu}}{dp_T d\eta}\Big)^{\bar{p}}}{\frac{dn^{pp}}{dp_T d\eta}\Big)^{\bar{p}}}$$

The ratio of raw counts is then equated with the ratio of differential yields in η and p_T, assuming that all corrections do cancel out. The ratio of raw counts was obtained with information from the Ring Imaging Cherenkov detector whose efficiency is high ($\sim 95\%$) but has not been included in this analysis. The errors shown for the nuclear modification factors of anti-protons and pions include the contributions from correlations between the parameters of the fits made to the ratios of raw counts. No attempt was made to estimate the contributions from anti-lambdas feed down to the anti-proton result. The remarkable difference between baryons and mesons has also been seen at RHIC energies around mid-rapidity, and has been related to parton recombination [17]. The same explanation could be offered for these high rapidity results, but it is difficult to imagine the existence of the thermal bath of partons at high rapidity in d+Au collisions.

At the time the invariant yields at $\eta = 3.2$ where shown for the first time [18], the clear difference between positive and negative charged particles, prompted some to associate the suppression seen in d+Au collisions at forward angles with the so called "beam fragmentation"
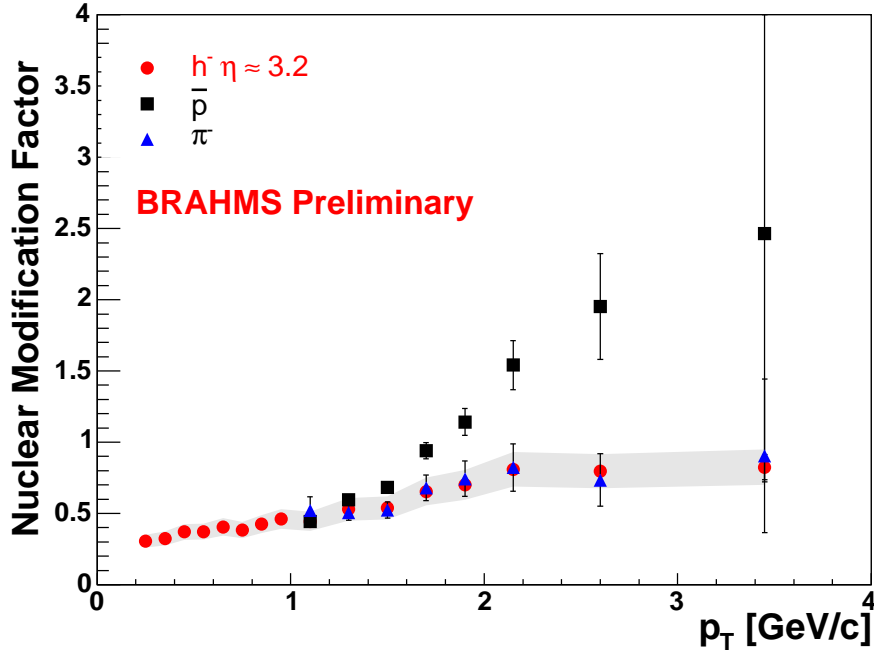
Figure 4. The nuclear modification factor R_{dAu} calculated for anti-protons (filled squares) and negative pions (filled triangles) at $\eta = 3.2$. The same ratio calcutated for negative particles at the same pseudo-rapidity [13] is shown with filled circles, and the systematic error for that measurement is shown as grey band.

[19]. More recent work based on NLO pQCD has indicated the difficulty in reconciling the data with the behavior of standard fragmentation functions [20]. Panel a of Fig. 5 shows that, there are as many protons as positive pions ($\sim 80\%$ at $p_T \sim 2 GeV/c$) in the positive particle distribution at $\eta = 3.2$. The abundance of baryons at this high energy and rapidity doesn't support the idea of baryon suppression in the fragmentation region [21, 22] where, because of their high energy, the quarks of the beam would fragment independently mostly into mesons. Panel b of the same figure shows that for all values of p_T, the fraction of negative pions is high and equal to 80%.

The suppression of particle production at mid-rapidity in Au+Au central collisions compared to incoherently added p+p interactions, or properly scaled disributions obtained from peripheral Au+Au collisions, is widely accepted as a necessary condition for momentum degradation by gluon radiation, as partons traverse an opaque medium before they hadronize. That momentum degradation is expected to be a function of the length of the parton's path inside the medium as well as the medium density [23]. In the above mentioned work, such partonic energy loss is encoded in a medium modified fragmentation function that has the standard (in vacuum) behavior, but only after the energy has been degraded by several interactions in the medium. These interactions are distributed in number according to a Poisson distribution with a mean value equal to $L/\sigma\rho$ where L is the parton's path length in the medium, σ is the interaction cross-section and ρ the medium density. The final fragmentation also includes the gluons radiated at each interaction. The pion rapidity density, which must be directly related to the medium density, changes by almost a factor of three between mid-rapidity and y = 3 (see Fig. 1). One would then expect less energy loss at y=3, by a comparable factor, but as can be seen in
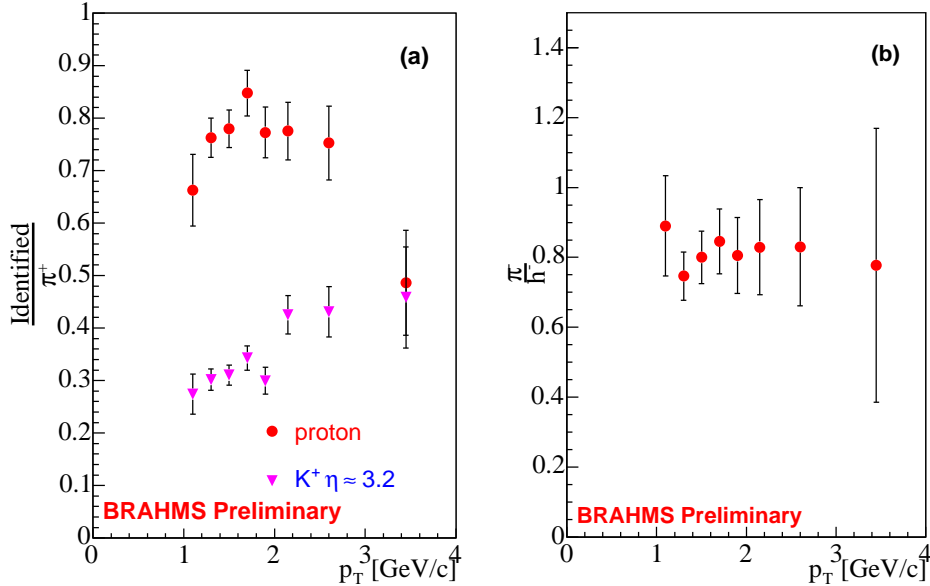
Figure 5. Some results with pid at $\eta = 3.2$: (a) Particle composition of positive charged hadrons at $\eta = 3.2$ (b) The fraction of negative hadrons identified as pions at the same pseudo-rapidity.

Fig. 6, there is no noticeable difference between the p_T suppressions at $\eta = 3.2$ and previous measurements at mid-rapidity and $\eta = 2.2$ [2]. This result may indicate the interplay between energy loss effects that get weaker at higher rapidities, and initial state related suppression that becomes stronger as the number of gluons in one of the Au ions is further reduced by gluon fusion. On the other hand, if the p_T distributions at forward rapidities are stepper than the ones measured at mid-rapidity, smaller energy losses would be magnified producing similar results as the measurements. Further analysis on this subject is currently in progress.

In summary, BRAHMS has studied the properties of bulk particle production as well as baryon number transport in Au+Au collisions at $\sqrt{s_{NN}} = 200 GeV/c$. We have also compared charged particle production in Au+Au and d+Au collisions to similar production in p+p collisions at the same energy. Such comparisons, show an strong suppression at intermediate transverse momentum that is associated with the formation of a dense and opaque medium. In d+Au collisions at the same energy, such suppression does not appear at mid-rapidity, but is present at forward rapidities and is even more pronounced in central collisions.

5. Acknowledgments

References
[1] K. Adcox *et. al.*, PHENIX Collaboration, Phys. Rev. Lett. **88** 022301 (2002); S. S. Adler *et. al.*, STAR Collaboration, Phys. Rev. Lett. **89** 202301 (2002); B.B. Back, *et. al.*, PHOBOS Collaboration, Phys. Lett. B **578**, 297 (2004).
[2] I. Arsene *et al.*, BRAHMS Collaboration, Phys. Rev. Lett. **91**, 072305 (2003).
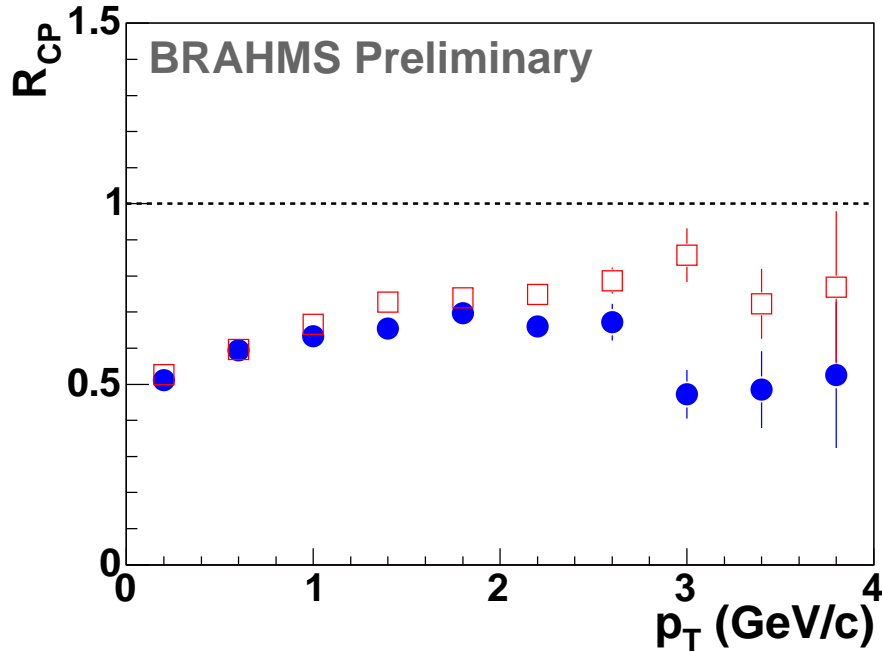[3] I. Arsene *et al.*, BRAHMS Collaboration, Nucl. Phys. A **757** 1-27, nucl-ex/0410020 (2004).

Figure 6. Rcp of charged particles from Au+Au at $\eta = 3.2$ Open squares: positives, filled circles: negatives.

[4] I. Arsene et al., submitted to Phys. Rev. C. nucl-ex/053010 (2005).

[5] M. Adamczyk *et al.*, BRAHMS Collaboration, Nuclear Instruments and Methods A **499** 437 (2003).

[6] Y.K. Lee *et al.*, Nuclear Instruments and Methods A **499** 437 (2003).

[7] I.G. Bearden *et. al.*, Accepted for publication Phys. Rev. Lett. (nucl-ex/0403050).

[8] I.G. Bearden *et al.* Phys. Rev. Lett. **93,** 102301 (2004).

[9] T. Hirano and Y. Nara, Nucl. Phys. A **743**, 305 (2004); T. Hirano and Y. Nara J. Phys. G**31**, S1, (2005).

[10] B.B. Back, *et. al.*, PHOBOS Collaboration, Phys. Rev. Lett. **89**, 222301, (2002).

[11] D. Kharzeev Phys. Lett. B **378**, 238-246, (1996).

[12] B.B. Back *et al.*, PHOBOS Collaboration, Phys. Rev. Lett. **91**, 72302 (2003); S.S. Adler *et al.*, STAR Collaboration, Phys. Rev. Lett. **91**, 72303 (2003); J. Adams *et al.*, PHENIX Collaboration, Phys. Rev. Lett. **91**, 72304 (2003).

[13] I. Arsene et al., Phys. Rev. Lett. **93**, 242303 (2004).

[14] D. Antreasyan *et al.*, Phys. Rev. D **19**, 764 (1979).

[15] L. McLerran and R. Venugopalan, Phys. Rev. D **49**, 2233 (1994), Phys. Rev. D **49**, 3352 (1994), Phys. Rev. D **50**, 2225 (1994), Phys. Rev. D **59**, 094002 (1999); Y. V. Kovchegov, Phys. Rev. D **54**, 5463 (1996), Phys. Rev. D **55**, 5445 (1997).

[16] D. Kharzeev, Y. V. Kovchegov and K. Tuchin Phys. Rev. D **68**, 094013, (2003), hep-ph/0307037; D. Kharzeev, E. Levin and L. McLerran, Phys. Lett. B **561**, 93 (2003); R. Baier, A. Kovner and U. A. Wiedemann Phys. Rev. D **68**, 054009, (2003); J. Albacete, *et. al.* hep-ph/0307179.; A. Dumitru and J. Jalilian-Marian, Phys. Lett. B **547**, 15 (2002); J. Jalilian-Marian, A. Kovner, A. Leonidov, H. Weigert, Phys. Rev. D **59**, 014014 (1999). J. Jalilian-Marian *et al.* Phys. Lett. B **577**, 54-60 (2003), nucl-th/0307022;

[17] R. C. Hwa, C. B. Yang and R. J. Fries Phys. Rev C**71**, 024902, (2005).

[18] R. Debbe (for the BRAHMS Collaboration) J. Phys. G **30** S759-S765, (2004).

[19] M. Gyulassy Proceedings RIKEN Workshop Volume **57**, 141 Dec. 2-6 (2003).

[20] V. Guzey, M. Strikman, W. Vogelsang, Phys. Lett. D **603**, 173 (2004).

[21] A. Dumitru, L. Gerland, and M. Strikman hep-ph/0211324, (2003).

[22] A. Berera *et al.* Phys. Lett. B **403**, 1-7, (1997).

[23] X. N. Wang and Z. Huang, Phys. Rev. C **55**, 3047, (1997).